



Mechanisms and feedback causing changes in upper stratospheric ozone in the 21st century

L. D. Oman,^{1,2} D. W. Waugh,¹ S. R. Kawa,² R. S. Stolarski,² A. R. Douglass,² and P. A. Newman²

Received 1 May 2009; revised 16 October 2009; accepted 27 October 2009; published 9 March 2010.

[1] Stratospheric ozone is expected to increase during the 21st century as the abundance of halogenated ozone-depleting substances decrease to 1960 values. However, climate change will likely alter this “recovery” of stratospheric ozone by changing stratospheric temperatures, circulation, and abundance of reactive chemical species. Here we quantify the contribution of different mechanisms to changes in upper stratospheric ozone from 1960 to 2100 in the Goddard Earth Observing System chemistry-climate model, using multiple linear regression analysis applied to simulations using either A1b or A2 greenhouse gas (GHG) scenarios. In both scenarios, upper stratospheric ozone has a secular increase over the 21st century. For the simulation using the A1b GHG scenario, this increase is determined by the decrease in halogen amounts and the GHG-induced cooling, with roughly equal contributions from each mechanism. There is a larger cooling in the simulation using the A2 GHG scenario, but also enhanced loss from higher NO_y and HO_x concentrations, which nearly offsets the increase because of cooler temperatures. The resulting ozone evolutions are similar in the A2 and A1b simulations. The response of ozone caused by feedback from temperature and HO_x changes, related to changing halogen concentrations, is also quantified using simulations with fixed-halogen concentrations.

Citation: Oman, L. D., D. W. Waugh, S. R. Kawa, R. S. Stolarski, A. R. Douglass, and P. A. Newman (2010), Mechanisms and feedback causing changes in upper stratospheric ozone in the 21st century, *J. Geophys. Res.*, *115*, D05303, doi:10.1029/2009JD012397.

1. Introduction

[2] One of the critical questions of Earth’s climate system is how ozone concentrations will evolve during the 21st century. The concentration of ozone-depleting substances (ODSs) increased rapidly during the 1960s to 1980s, peaked in the 1990s, and is expected to decrease almost back to 1960s levels by the end of this century. As the abundance of stratospheric halogens returns to 1960s values, stratospheric ozone, if there were no other changes, would be expected to increase back to 1960s values. However, the concentrations of greenhouse gases (GHGs) are expected to continue to increase, causing other changes in the thermal, dynamical, and chemical structure of the stratosphere. These changes could alter the “expected” recovery of stratospheric ozone by a variety of mechanisms. For example, the upper stratosphere is expected to continue to cool because of the continued increase of CO_2 . This cooling will slow the rate of

gas-phase reactions that destroy ozone and hence increase ozone concentrations [e.g., Haigh and Pyle, 1979; Brasseur and Hitchman, 1988; Shindell et al., 1998; Rosenfield et al., 2002]. Increases in N_2O and CH_4 could also impact the recovery of ozone by increasing nitrogen and hydrogen ozone-loss cycles [e.g., Randeniya et al., 2002; Rosenfield et al., 2002; Chipperfield and Feng, 2003; Portmann and Solomon, 2007]. Increases in GHGs have also been linked to changes in stratospheric transport that could impact the ozone recovery [Waugh et al., 2009; Li et al., 2009].

[3] Projections of the ozone evolution in the 21st century use models that couple stratospheric chemistry and climate. Before *World Meteorological Organization (WMO)* [2007], global ozone projections were made primarily with two-dimensional (2-D) models, most of which did not include coupling between future temperature changes and the chemistry. Some projections were made with 2-D models including this coupling [e.g., Rosenfield et al., 2002; Chipperfield and Feng, 2003; Portmann and Solomon, 2007]; however, these models did not fully capture circulation changes because of changes in wave driving from the troposphere or changes in the polar vortices. More recently, three-dimensional models that include full representations of dynamical, radiative, and chemical processes in the atmosphere, and the couplings between these processes, have been developed, and these chemistry-climate models

¹Department of Earth and Planetary Sciences, Johns Hopkins University, Baltimore, Maryland, USA.

²Atmospheric Chemistry and Dynamics Branch, NASA Goddard Space Flight Center, Greenbelt, Maryland, USA.

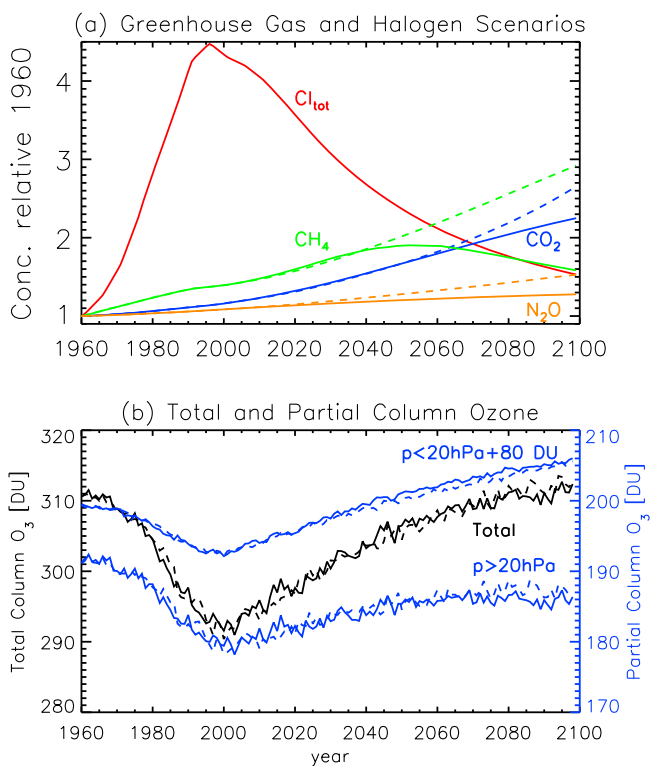


Figure 1. Temporal variation of (a) surface GHGs and halogens (solid line, A1b; dashed line, A2) and (b) total or partial column ozone averaged between $60^\circ S$ and $60^\circ N$ (solid line, A1b; dashed line, A2), between 1960 and 2100.

(CCMs) have been used to make projections of ozone through the 21st century [e.g., Austin and Wilson, 2006; Eyring et al., 2007; Shepherd, 2008].

[4] While there have been detailed analyses of the simulated ozone in these CCMs, there has been rather limited quantitative attribution of these ozone changes to the different mechanisms. Although several studies have attributed increases in upper stratospheric ozone and decreases in lower stratosphere ozone to cooling and circulation changes, respectively [e.g., Eyring et al., 2007; Shepherd, 2008; Li et al., 2009], the relative role of the different mechanisms has not been quantified. Newchurch et al. [2003] examined 10 years of Halogen Occultation Experiment (HALOE) observations to attribute changes in ozone to different mechanisms, but it was limited by the time period and available observations of trace gases. Quantitative attribution has been performed for some CCMs with simulations using either fixed GHGs [e.g., WMO, 2007] or fixed ODSs [e.g., Waugh et al., 2009]. However, such analysis does not isolate the relative role of different GHG-related mechanisms in causing changes in ozone. This attribution is needed to understand exactly how changes in different GHGs will impact stratospheric ozone. There are often multiple mechanisms by which an increase in a GHG can impact ozone, and the sign of the ozone changes are not necessarily the same for each mechanism. Without knowledge of the relative role of different mechanisms, it is difficult to know how ozone projections will change for different GHG scenarios (e.g., whether the GHG impact on ozone will simply scale with GHG concentrations). This is important because

the recent CCM projections of the 21st century have all used the same GHG scenario [Eyring et al., 2007], and there have not been comparisons of projections for different scenarios (other than the unrealistic case of fixed GHGs).

[5] Here we use multiple linear regression (MLR) to estimate the relative contribution of changes in halogens, temperature, reactive nitrogen (NO_x), and reactive hydrogen (HO_x) to changes in the simulated ozone from the NASA Goddard Earth Observing System (GEOS) CCM [Pawson et al., 2008]. We consider simulations using two different scenarios of future GHG emissions: the Intergovernmental Panel on Climate Change (IPCC) [2001] A1b scenario that has been used in most recent CCM simulations and the A2 scenario that has larger increases in all GHGs. Even though there are significant differences in the GHG concentrations in the latter half of the 21st century, the ozone changes in these two simulations are very similar. The MLR indicates that the net changes in upper stratospheric ozone are similar because of the compensating effects of larger cooling and larger abundances of reactive nitrogen and hydrogen in the simulation with larger GHG changes.

[6] The model, simulations, and evolution of ozone in the GEOS CCM simulations are described in the next section. The simulated changes in ozone and quantities that can impact ozone are described in section 3. Methods used in the analysis are presented in section 4. Then in section 5, we quantify the relative contribution of different mechanisms to ozone changes in the upper stratosphere. Section 6 compares the results to a fixed-halogen simulation, and concluding remarks are given in section 7.

2. Model

[7] We consider here GEOS CCM [Pawson et al., 2008] simulations of the past (1960–2004) and future (2000–2100). The past simulations use the observed Hadley sea surface temperatures (SSTs) and sea ice data set from Rayner et al. [2003], whereas the future simulations use SSTs and sea ice output from AR4 integrations of the National Center for Atmospheric Research Community Climate System Model, Version 3 for both the IPCC [2001] A1b and A2 GHG scenarios. Observed surface concentrations of GHGs and halogens are used for past simulations. Future simulations use the A1b or A2 scenario for surface concentrations of GHGs and the WMO [2003] Ab scenario for surface concentrations of halogens. The time series of the surface concentrations of the GHGs and total chlorine, normalized by their 1960 values, are shown in Figure 1a. The two GHG scenarios are fairly similar until about 2040, when the A2 scenario shows faster increases of CO_2 and N_2O . CH_4 continues to increase in this scenario whereas it peaks around 2050 in the A1b scenario.

[8] Comparisons of the simulated temperature, ozone, water vapor, and other constituents with observations have been discussed by Pawson et al. [2008], Eyring et al. [2006, 2007], and Oman et al. [2008]. These studies have shown that GEOS CCM performs reasonably well compared to observations. Two noted deficiencies are a high bias in total O_3 at high latitudes when chlorine loading is low (in the 1960s) and the late breakup of the Antarctic polar vortex [Pawson et al., 2008].

[9] There is a 5 year overlap (2000–2004) in the above two simulations. In the analysis presented below, we join the simulations together in January 2001 to form a single time series from January 1960 to December 2099. We use “A1b” to denote the combination of the first reference past simulation (P1) and the A1b future simulation and “A2” for the combination of the second reference past (P2) and A2 future simulation. The P2 simulation is a second ensemble member of P1, varying only in initial conditions [Oman *et al.*, 2009]. A small discontinuity at January 2001, apparent in the time series for some quantities at some locations, does not impact results presented here. Below when we refer to a single simulation, we are referring to the composite past and future simulations joined in January 2001.

3. Modeled Changes 1960 to 2100

[10] Before examining the mechanisms responsible for ozone changes, we examine the changes in ozone and the quantities that can impact ozone changes in the GEOS CCM simulations, focusing on the long-term changes between 1960 and 2100 for the two simulations. Evolution of the 60°S–60°N average total column ozone and the partial columns above and below 20 hPa is similar for the A1b (solid lines) and A2 (dashed lines) simulations (Figure 1b).

[11] In both simulations, column ozone (black curves) decreases from 1960 to around 2000 and then increases back to values similar to 1960 by 2100. This evolution of total column ozone is qualitatively similar to that of the negative of the tropospheric total chlorine (Figure 1a), except the total chlorine peaks a few years earlier and has not quite returned to 1960 values by 2100. Although the extrapolar total column ozone in 2100 is similar to that in the 1960s, this is not necessarily the case for the ozone mixing ratio at a given location. In general, upper stratospheric ozone in the 2090s exceeds the 1960s values whereas the opposite is true for lower stratospheric ozone. This can be seen in the evolution of partial columns of ozone above and below 20 hPa (Figure 1b) (note that 80 Dobson units were added to the partial column above 20 hPa for graphical purposes).

[12] Further details of the differences in long-term evolution are shown in Figures 2a and 2b, which show the change in decadal-averaged ozone between the 1960s and 2090s for the -A1b (Figure 2a) and A2 (Figure 2b) simulations. Here and below, “1960s” ozone refers to the ozone averaged over the years 1960 to 1969, and “2090s” ozone is the average from 2090 to 2099. These plots show that in both simulations, the decadal-averaged 2090s extrapolar ozone is larger than that in the 1960s in the upper stratosphere, similar to that in the 1960s in the midstratosphere, and less than that in the 1960s in the lower stratosphere.

[13] As discussed in the Introduction, a number of mechanisms can influence the evolution of ozone concentrations in the stratosphere. To help understand the changes in ozone between the 1960s and 2090s, we show in Figures 2c–2l the change between the 1960s and 2090s in several quantities that influence ozone. As shown in Figures 2c and 2d, equivalent effective stratospheric chlorine (EESC) (where $EESC = Cl_y + \alpha Br_y$, with $\alpha = 5$) in the 2090s has returned to values similar to those in the 1960s in the lower stratosphere and is only around

0.3–0.5 ppb larger in the upper stratosphere (compare to the peak EESC values of around 3–4 ppb in 2000). (We use $\alpha = 5$ in the definition because Daniel *et al.* [1999] showed this is an appropriate value for the upper stratosphere, which is the focus of this study.) As a result, changes in EESC only make a minor contribution to the 1960–2100 changes in ozone (see below). This is not necessarily the case, however, for temperature, NO_y , HO_x , and residual vertical velocity. In both simulations, there is stratospheric cooling (Figures 2e and 2f), associated primarily with increasing concentrations of GHGs. The A2 simulation shows the largest cooling consistent with the higher GHG concentrations in this scenario (see Figure 1a). This larger cooling in the A2 simulation alone causes slower destruction of ozone and larger increases in ozone compared to the A1b simulation. However, as discussed above, the net ozone is similar in the A1b and A2 simulations, implying that other compensating changes in ozone are occurring.

[14] Two other mechanisms important for changes in ozone concentrations are changes in nitrogen and hydrogen ozone-loss cycles. Figures 2g–2j show that the magnitude of changes in NO_y and HO_x between the 1960s and 2090s are different in the A1b and A2 simulations, with a larger increase in upper stratospheric NO_y and HO_x in the A2 simulation (again, consistent with higher GHG concentrations in this scenario; see Figure 1a). It is important to note that changes in HO_x and NO_y do not simply follow changes in CH_4 and N_2O , respectively. This can be seen by comparing Figures 2g and 2i with Figure 1a: there are negative changes in some areas in NO_y and HO_x from the 1960s to 2090s despite large increases in N_2O and CH_4 . The difference between HO_x and CH_4 trends is because methane oxidation is not the only source of stratospheric H_2O ; changes in the tropical tropopause cold point also influence stratospheric H_2O [Oman *et al.*, 2008]. HO_x formation can be influenced additionally by changes in ultraviolet radiation and ozone concentration. $NO_y - N_2O$ trend differences occur because the loss of NO_y is influenced by temperature [Rosenfield and Douglass, 1998] and also could be affected by circulation changes.

[15] Changes in transport also influence the ozone evolution, and Figures 2k and 2l show the change in residual vertical velocity, as a proxy for circulation changes. There is a similar increase in the tropical vertical velocity between the 1960s and 2090s in the two simulations, with a slightly larger change in the A2 simulation.

[16] In summary, Figure 2 shows that there are larger changes in temperature, NO_y , and HO_x in the A2 simulation, but the ozone change is similar in the two simulations. This suggests compensating ozone changes caused by different mechanisms, which is quantified below.

4. Linear Regression Analysis

[17] We want to estimate the contribution of the different mechanisms to the simulated changes in ozone. The principal analysis method used to do this is MLR. For a given location and time, MLR is applied to determine the coefficients m_X such that

$$\Delta O_3(t) = \sum_j m_{X_j} \Delta X_j(t) + \varepsilon(t), \quad (1)$$

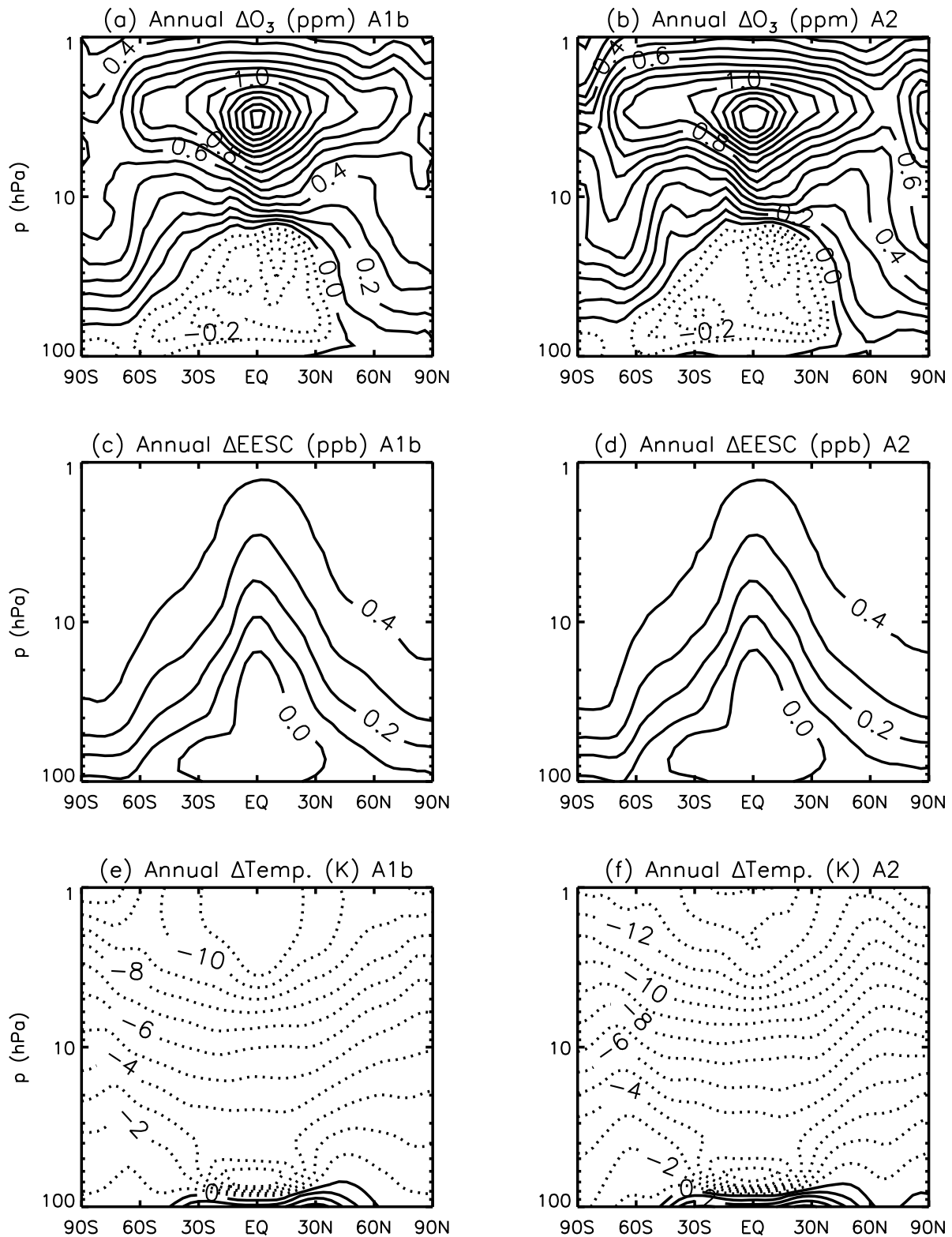


Figure 2. Difference in ozone (parts per million) between the 1960s and 2090s for (a) annual A1b scenario and (b) annual A2 scenario. Also shown for the same time period are changes in (c) EESC (parts per billion (ppb)) for A1b, (d) EESC (ppb) for A2, (e) temperature (kelvin (K)) for A1b, and (f) temperature (K) for A2. The difference in annual NO_y (ppb) between the 1960s and 2090s is shown for (g) A1b scenario, (h) A2 scenario, (i) HO_x (parts per trillion (ppt)) for A1b, (j) HO_x (ppt) for A2, (k) \bar{w}^* (millimeter per second (mm/s)) for A1b, and (l) \bar{w}^* (mm/s) for A2.

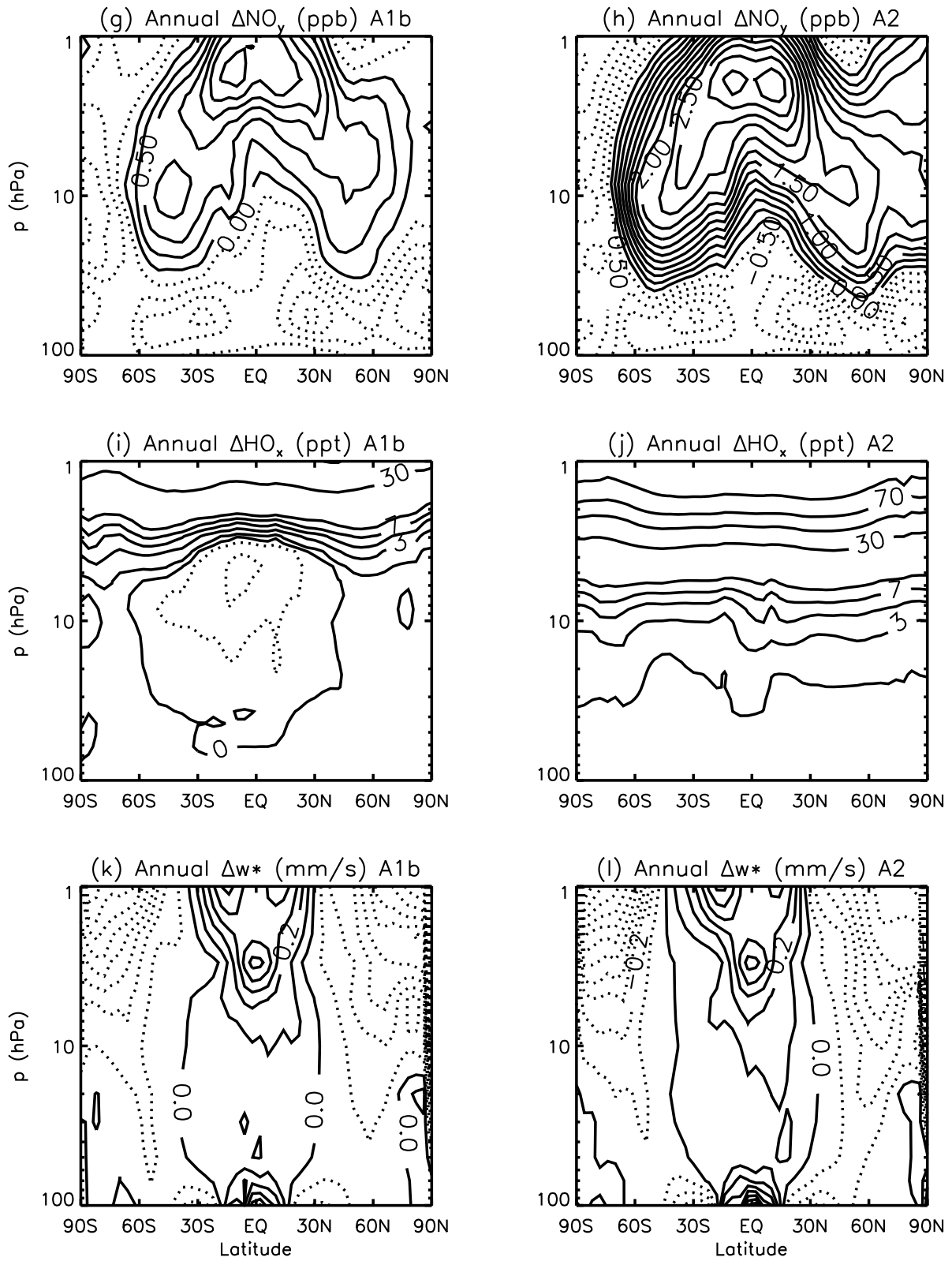


Figure 2. (continued)

where the X_j are the different quantities that could influence ozone, the coefficients m_X are the sensitivity of ozone to the quantity X , i.e., $m_X = \partial O_3 / \partial X$, and ε is the error in the fit. MLR analysis has been applied extensively to observations or simulations to isolate a long-term linear trend in ozone (and, more recently, long-term variations in ozone correlated with EESC) [e.g., *WMO*, 2007, and references therein].

[18] To apply equation (1), we need to decide which mechanisms we want to isolate and the quantities X_j that are the “proxies” for these different mechanisms. In the MLR calculations presented below, we focus on ozone changes caused by changes in halogen, nitrogen, and hydrogen ozone-loss cycles as well as changes in temperature. To do this, four explanatory variables (X_j) are used in equation (1): EESC, reactive nitrogen ($\text{NO}_y = \text{NO} + \text{NO}_2 + \text{NO}_3 + 2^* (\text{N}_2\text{O}_5) + \text{HNO}_3 + \text{HO}_2\text{NO}_2 + \text{ClONO}_2 + \text{BrONO}_2$), reactive hydrogen ($\text{HO}_x = \text{OH} + \text{HO}_2$), and temperature (T). Each term on the right-hand side of equation (1) then gives the “contribution” of the response in ozone due to a change in X and the role the corresponding mechanism plays in the ozone evolution (i.e., $m_{\text{EESC}}\Delta\text{EESC}$ is the contribution due to changes in EESC and the role of changes in halogen ozone-loss cycles). We chose HO_x as an explanatory variable rather than H_2O , even though it is a shorter-lived species, to address feedbacks that are discussed in section 6 that would not be seen using H_2O .

[19] Rather than using the above four quantities as explanatory variables X in the MLR analysis, an alternative approach would be to use the surface concentrations of the ODSs and GHGs as the independent variables X . *Stolarski et al.* [2010] used this approach when examining temperature changes in the GEOS CCM simulations considered here. Also, *Shepherd and Jonsson* [2008] used ODSs and CO_2 to separate their impact on temperature and ozone changes but could not quantify the impact of other GHGs, although they are likely to have a smaller impact. However, as discussed above, changes in HO_x and NO_y do not simply follow changes in CH_4 and N_2O , respectively, and regressing against CH_4 and N_2O will not necessarily isolate the role of changes in the hydrogen and nitrogen cycles in the response of ozone. Furthermore, the time series of CO_2 and N_2O are not independent in terms of correlation for either scenario, and neither are CO_2 and CH_4 for the A2 scenario (see Figure 1). This means that the MLR could not separate the impact of these fields.

[20] The model output used in the MLR analysis is from instantaneous output from the first day of each month since not all variables were saved as monthly averages; however, using monthly mean data should not materially affect the results. This analysis was done for individual months as well as annual averages. Here we focus on presenting results calculated using annual averages. Thus, we examine inter-annual and longer time scale variations in ozone. The above MLR analysis presented below uses all 140 years of the GEOS CCM simulations to determine the coefficients m_X . Calculations using shorter time periods (i.e., different start or end dates) show some sensitivity to the period used (e.g., if the start date is between 1960 and 1990 and the end date is between 2050 and 2100, there is some variation in the coefficients).

[21] There are several complications with the above linear regression approach. First, other mechanisms that are not

considered in the regression (e.g., transport) could play a role. Second, significant correlations can exist between the temporal variations of the quantities, i.e., the quantities are not necessarily independent. Third, a high correlation between ozone and a quantity does not show causality, as ozone could be causing the quantity to change, or changes in another quantity could be causing both ozone and the quantity of interest to change in a correlated way. Temperature and ozone in the upper stratosphere is an example of this third complication: changes in ozone cause, through changes in short-wave heating, changes in temperature. At the same time, changes in temperature cause, through changes in reaction rates, differences in the response of ozone. Also, the relationship between the variables we use and ozone may not be linear. Because of the above complications, caution must be applied when interpreting the MLR results presented below. Additional discussion and analysis of these issues is included below.

5. Relative Contributions to Ozone Changes

[22] We now use the MLR analysis described in section 4 to quantify the role of different mechanisms in causing the ozone changes in the A1b and A2 simulations. We first examine the ozone evolution in the tropical upper stratosphere. As discussed above, the simulated upper stratospheric ozone in the 2090s is greater than in the 1960s. Examples are shown in Figures 3a and 3b, where the simulated evolution of annually averaged ozone over 10°S – 10°N at 2.9 hPa, for the A1b and A2 simulations, respectively, are shown (black curves). This shows that the ozone decreases rapidly from 1960 to 2000 and then increases, at roughly the same rate, back to 1960s values by the 2030s. The ozone continues to increase, although at a slower rate, and by the end of the century, the ozone is significantly higher ($\approx 20\%$) than in the 1960s.

[23] From the MLR analysis, it is possible to estimate the contribution of different mechanisms to the changes in ozone. Specifically, the coefficients m_X from equation (1) are multiplied by the simulated change in each quantity ΔX to determine the contribution to the change in ozone (i.e., $m_{\text{EESC}}\Delta\text{EESC}$ is the contribution due to changes in EESC). The individual contributions for each quantity are shown for A1b (Figure 3c) and A2 (Figure 3d), and the ozone calculated from the sum of these contributions added to the mean ozone value (dotted black lines) are shown as the magenta curves in Figures 3a and 3b. There is excellent agreement between this “reconstruction” and the simulated ozone change. In the A1b simulation in Figure 3c, the long-term evolution of ozone at 2.9 hPa is dominated by changes in EESC (red curve) and T (blue curve), with negligible contributions from variations in NO_y (orange curve) and HO_x (green curve). The situation is somewhat different for the A2 scenario, where there is a larger trend in T , NO_y , and HO_x at this level and changes in NO_y and HO_x now contribute to the ozone change. However, the decrease in O_3 due to the increase in NO_y and HO_x is canceled out by the larger increase caused by the larger T trend, and the net O_3 change in A2 is similar to that of A1b.

[24] Figures 3a and 3b show that the ozone reconstruction from the MLR analysis using T , EESC, NO_y , and HO_x reproduces the simulated ozone evolution in the tropics at

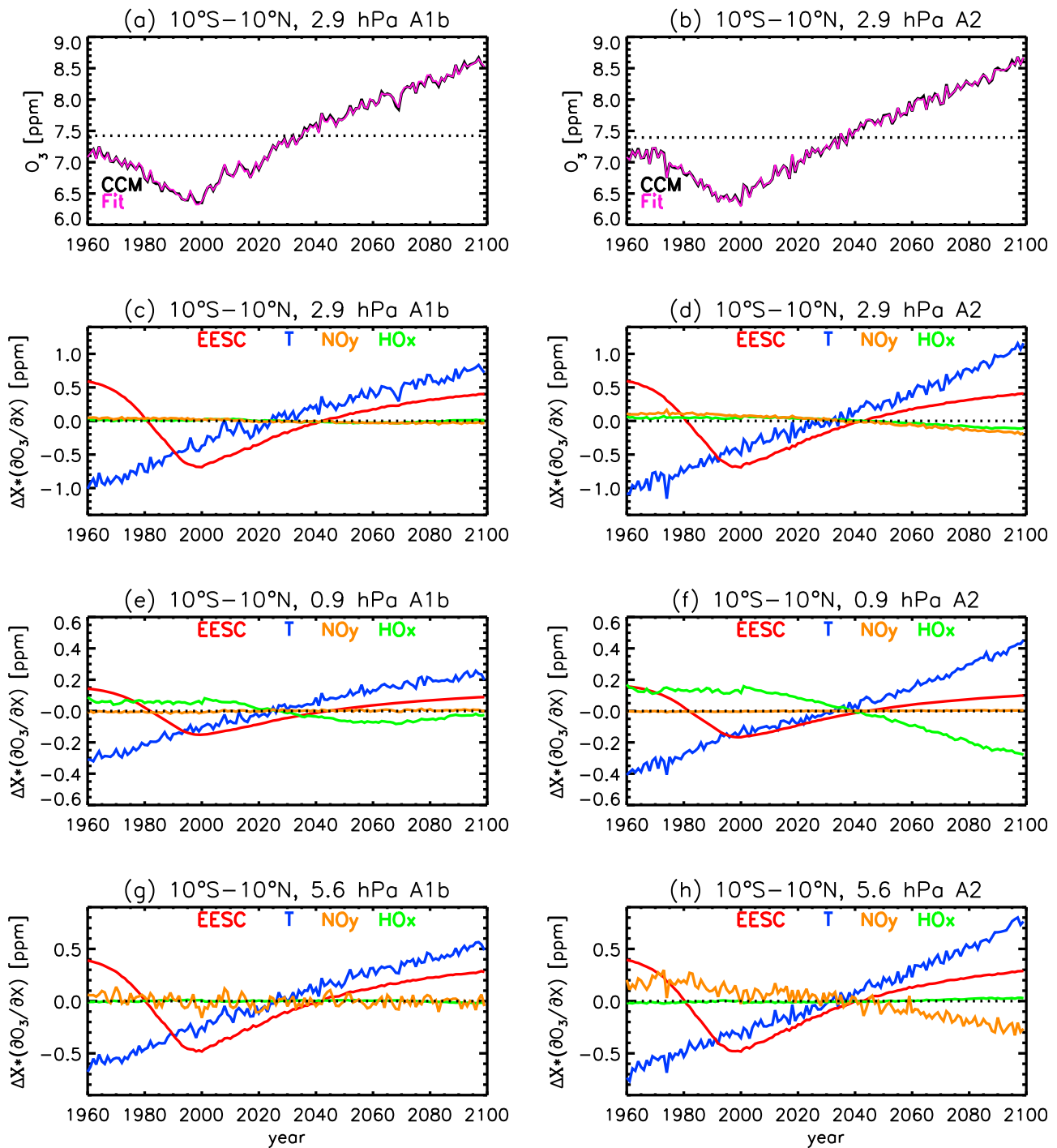


Figure 3. Evolution of annual average ozone at 2.9 hPa, 10°S–10°N for (a) A1b and (b) A2. Also shown is the contribution of different mechanisms for (c, d) 2.9 hPa, (e, f) 0.9 hPa, and (g, h) 5.6 hPa for each scenario.

2.9 hPa. However, this good agreement may not apply throughout the stratosphere. To assess how well the model ozone variability is explained by the MLR analysis, the square of the correlation coefficient between the MLR reconstruction and simulated ozone is shown for the original time series (Figure 4a) and a filtered time series with low-frequency variability removed (Figure 4b). Since significant autocorrelation exists over many locations in the original

time series, we focus on the time series in Figure 4b, which does not have significant autocorrelations. Figure 4b shows that the fit between the MLR analysis and simulated ozone is very good in the extrapolar upper stratosphere (e.g., in the tropical upper stratosphere, over 90% of the interannual variability is explained by the MLR analysis), but the fit is a lot poorer in polar regions and in the middle and lower stratosphere. This poorer fit is most likely attributable to the

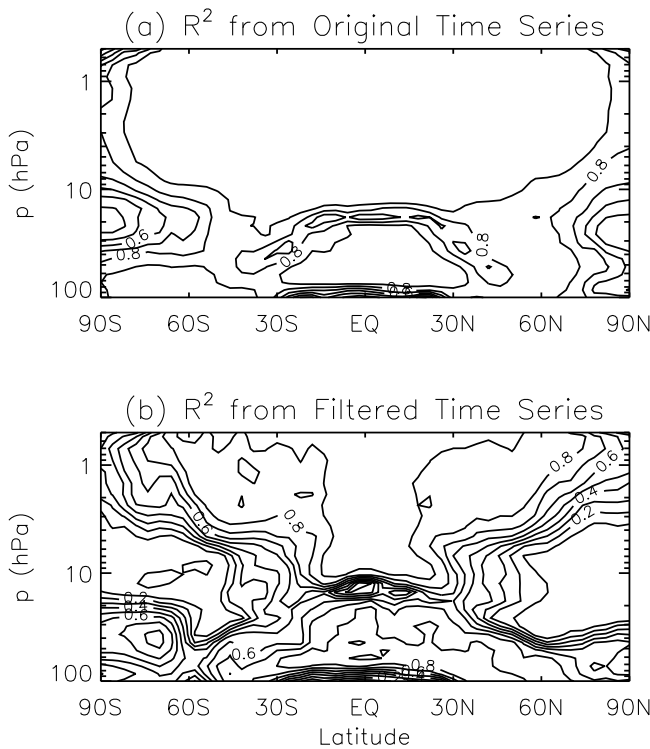


Figure 4. Annual correlation coefficient squared for (a) the original model ozone time series and MLR fit and (b) a filtered time series with low-frequency variability removed by applying a 1:2:1 filter iteratively 30 times to each quantity.

larger role of transport, which is not explicitly accounted for in the MLR analysis. Because of the above, we focus our MLR analysis on ozone changes in the extrapolar upper stratosphere.

[25] The analysis at 2.9 hPa indicates that changes in NO_y and HO_x make negligible contributions to ozone changes for the A1b simulation, but NO_y and HO_x do make significant contributions for the A2 simulation. However, the contributions of the different quantities vary with altitude. This is illustrated in Figures 3e–3h, which show the contributions for 0.9 and 5.6 hPa. (The simulated ozone and MLR reconstruction are not shown as the evolution and agreement is similar to that for 2.9 hPa.) At 0.9 hPa (Figures 3e and 3f), HO_x -related ozone loss is more important than at 2.9 hPa. This is especially evident in the A2 scenario (Figure 3f) in which there is a much larger CH_4 trend yielding a larger HO_x trend. The larger HO_x -related ozone loss is again offset by larger T contributions. In contrast to 0.9 hPa, NO_y -related ozone loss is important at 5.6 hPa for the A2 scenario (Figure 3h). In the A1b simulation, NO_y variations contribute to year-to-year variability but not to the long-term trend (Figure 3g), whereas in the A2 simulation, variations in NO_y contribute to the long-term behavior (Figure 3h). The trend caused by increased NO_y results in an ozone decrease of 0.5 ppm from the 1960s to the 2090s. As with the larger changes in T and HO_x at 0.9 hPa, the larger changes in T and NO_y in the A2 simulation at 5.6 hPa cause larger changes in ozone, but these changes are of opposite sign, and the net change in ozone in A2 is similar to that in the A1b simulation.

[26] Close inspection of Figures 3c–3h shows the relative contributions of the different mechanisms to changes in ozone vary with time. This is quantified in Figure 5, which shows the vertical variation of the changes in tropical ozone and individual contributions of different mechanisms for the A1b (solid curves) and A2 (dashed curves) simulations, over 1960–2000 (Figure 5a), 2000–2100 (Figure 5b), and 1960–2100 (Figure 5c).

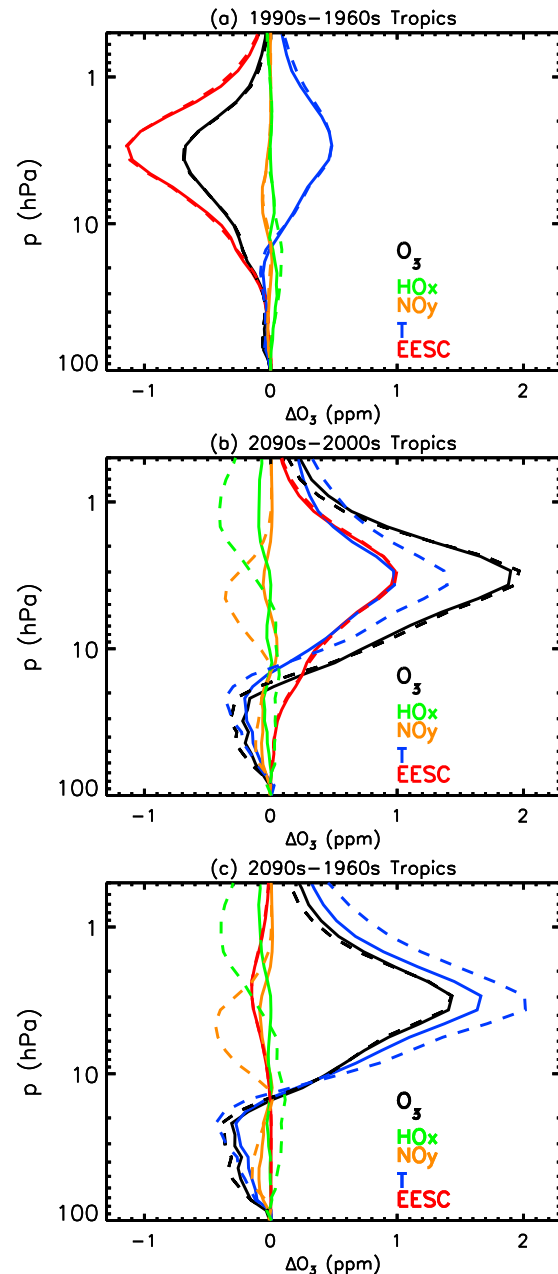


Figure 5. Vertical variation of changes in ozone (solid black curve) and individual contribution of different mechanisms for annual averages over the tropics. The changes are for (a) 1990s minus 1960s P1 (solid curve) and P2 (dashed curve), (b) 2090s minus 2000s A1b (solid curve) for A2 (dashed curve) scenario, and (c) 2090s minus 1960s A1b (solid curve) for A2 (dashed curve) scenario.

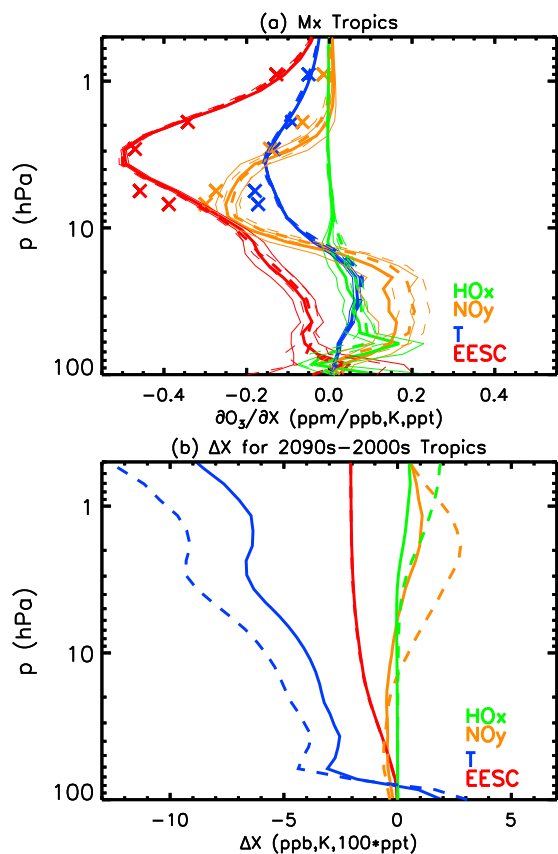


Figure 6. (a) Sensitivities of ozone to various factors (thick curves) and 3σ confidence intervals (thin curves) for annual averages over the tropics (10°S – 10°N) with the overplotted crosses showing the chemical box model calculations and (b) the 2090s minus 2000s change in T , EESC, and NO_y and HO_x divided by 100 for A1b (solid curves) and A2 (dashed curves). The reference 2000s are an average of 2000–2009.

[27] Over the 1960–2000 period, both simulations have identical forcings and only vary by the initial conditions, so very similar changes occur in each simulation. The largest change in ozone (-0.6 ppm) occurs in the upper stratosphere at ~ 3 hPa. This change is mostly caused by the increasing levels of EESC (-1.1 ppm) and is somewhat offset by the decreasing temperature (0.5 ppm). The cooling of the upper stratosphere is mostly due to increases in GHGs such as CO_2 but also caused by decreased ozone (see section 6). Over the last 40 years, NO_y and HO_x increases make an insignificant contribution to ozone changes in the upper stratosphere. The ozone changes in the lower stratosphere are much smaller than in the upper stratosphere and are discussed briefly below.

[28] The ozone change over the 21st century (2000s to 2090s) is very different from 1960 to 2000: upper stratospheric ozone increases over this period because of decreases in EESC and decreases in T (Figure 5b). There are very similar ozone evolutions for the two different scenarios, but the contributions from the different mechanisms vary. As discussed above, there is a larger positive increase in upper stratospheric ozone due to temperature changes in A2 than in A1b because of larger temperature decreases

in A2. These increases are almost entirely balanced by increased loss from NO_y and HO_x increases, with losses due to NO_y largest between 10 and 3 hPa and those due to HO_x largest above 5 hPa (consistent with results of Portmann and Solomon [2007]), resulting in very similar ozone evolutions.

[29] Figure 6a shows that the m_X calculated from the two simulations are very similar, implying that the differences in contributions in the two simulations are due to differences in the temperature and composition (Figure 6b) rather than differences in the sensitivities. The 3σ confidence intervals of the sensitivities are also shown in Figure 6a (thin curves), and these indicate that uncertainties with this analysis are generally largest in the lower portions of the stratosphere, while in the upper portions, the confidence intervals are much smaller with the largest uncertainty associated with the calculated NO_y sensitivities. The cooling with respect to the 2000s (defined as 2000–2009 average) values in A2 is significantly larger (2 – 4 K) (Figure 6b), causing a larger increase in the middle and upper stratospheric ozone. The differences in NO_y and HO_x are also larger in the A2 simulation (Figure 6b), consistent with the increased levels of N_2O and CH_4 , respectively, shown in Figure 1a. As discussed above, the increases in NO_y and HO_x are not necessarily the same as those in N_2O and CH_4 . For example, the increase in middle-upper stratospheric NO_y is much smaller than the increase in tropospheric N_2O , due to cooling in the middle and upper stratosphere, which increases NO_y loss [Rosenfield and Douglass, 1998]. Also, the NO_y -related ozone loss rates are only weakly dependent on T [e.g., Jonsson *et al.*, 2004], so the temperature decrease does not cause a significant difference in this loss.

[30] The changes over the complete period of the simulations (1960s to 2090s) are shown in Figure 5c. These are similar to the 21st century change (Figure 5b), except there is only a small contribution for EESC over the complete period, and ozone changes are dominated by the T changes.

[31] Although we focus here on upper stratospheric ozone changes, we briefly comment on the decrease in the tropical lower stratospheric ozone (Figure 5). Although the MLR analysis attributed most of this decrease to changes in T , the ozone responses are primarily due to increases in tropical upwelling. An increase in tropical upwelling in the lower stratosphere will, if no other changes occur, result in a decrease in ozone. Furthermore, increases in the upwelling and decreases in ozone will both lead to a decrease in temperature (through adiabatic cooling and reduced heating, respectively) and hence produce correlated changes in ozone and temperature. The larger upwelling increases and tropical lower stratospheric ozone decreases in A2 are consistent with larger increases in SSTs within the A2 simulation [Oman *et al.*, 2009]. The relationship between upwelling and decreases in tropical lower stratospheric ozone concentrations have been the focus of some recent studies, including those by Shepherd [2008] and Li *et al.* [2009].

[32] The ozone changes and contributions from relative mechanisms for middle latitudes are similar to that for the tropical stratosphere (e.g., compare Figure 7 and Figure 5). In the midlatitudes of both hemispheres (30° – 50° north and south), there is a decrease in the upper stratospheric ozone from the 1960s to 1990s due to increases in EESC (with a small compensating increase attributable to cooling), while

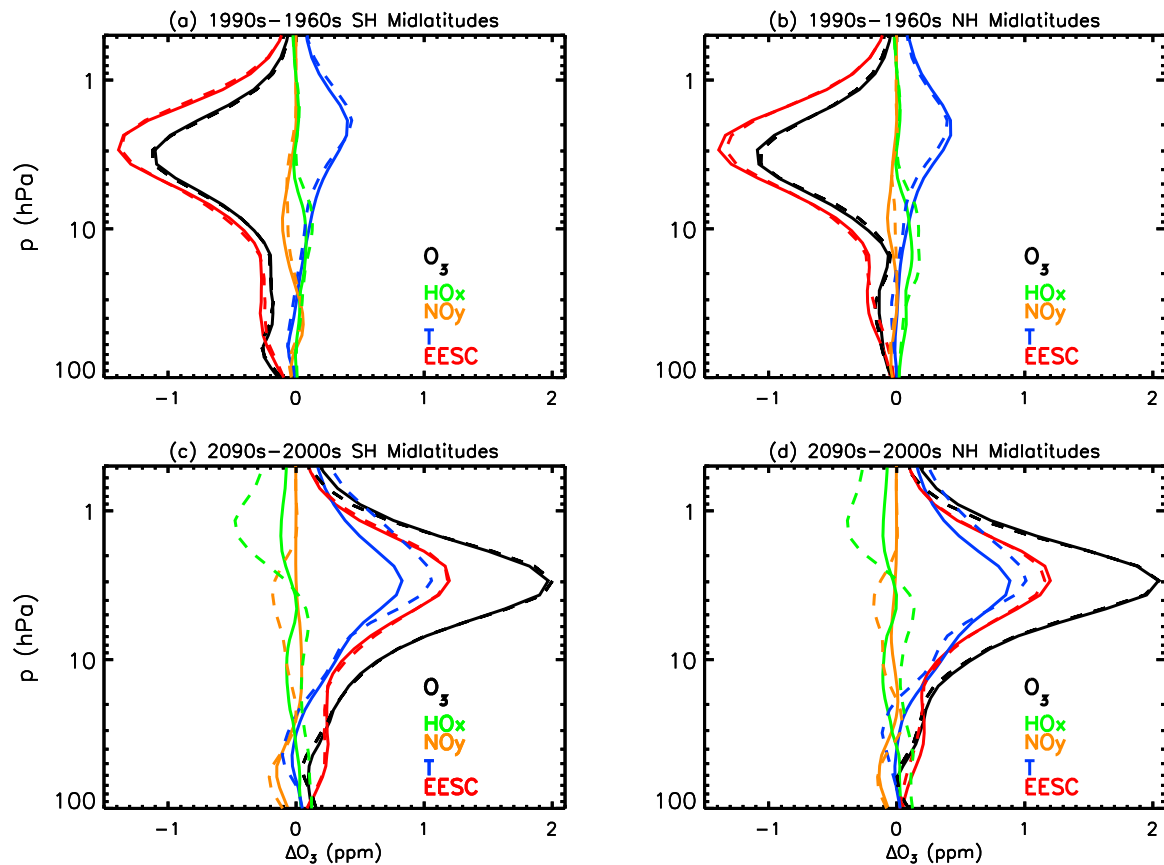


Figure 7. Vertical variation of changes in ozone (solid black curves) and individual contribution of different mechanisms for annual averages over (a, c) 50°S–30°S and (b, d) 30°N–50°N. The changes are for the 1990s minus 1960s P1 (solid curves) and P2 (dashed curves) scenario (Figures 7a and 7b) and 2090s minus 2000s A1b (solid curves) for A2 (dashed curves) scenario (Figures 7c and 7d).

the upper stratospheric ozone is projected to increase over the 21st century due to increases in EESC and further cooling (Figure 7). As in the tropics, the larger ozone increase in the A2 simulation is caused by larger cooling, which is canceled by larger ozone losses related to larger changes in NO_y and HO_x in the A2 simulation.

6. Fixed-Halogen Simulation

[33] Two questions that arise when using the MLR analysis are as follows: (1) How representative are the calculated sensitivities (i.e., can they be applied to other simulations)? (2) Can the MLR represent some of the feedback that occurs in the climate system (i.e., separating the effect of CO_2 on T from that caused by O_3 loss from EESC)? To examine these issues, we use an additional GEOS CCM simulation with the same SSTs and GHGs as the A1b simulation, but with halogens fixed at 1960 levels. As discussed by *Waugh et al.* [2009], the difference in ozone between the A1b and “fixed-halogen” simulations is the change in ozone due to EESC, with this EESC-induced change including both the direct EESC chemical impact and any “indirect” feedback.

[34] We first test whether the regression coefficients (sensitivities) m_X calculated above can be used to reconstruct the ozone in the fixed-halogen simulation. As above, we multiply the coefficients by the change in each quantity

(e.g., EESC, T , NO_y , HO_x) to determine the individual contributions to the ozone change and compare the sum of these contributions with the simulated ozone change. Figure 8a shows the evolution of tropical upper stratospheric (10°S–10°N at 2.9 hPa) ozone from the A1b and fixed-halogen simulations, together with the reconstructed ozone (using the coefficients m_X calculated from the A1b simulation for both reconstructions). There is good agreement between the simulated and reconstructed ozone for the fixed-halogen simulation, showing that the coefficients calculated here can be applied to different simulations.

[35] We now examine the direct and indirect EESC impact on ozone. *Waugh et al.* [2009] discussed the difference in ozone between the A1b and fixed-halogen simulations. This net change in ozone is due to EESC, with this EESC-induced change including both the direct EESC chemical impact and any indirect feedback. Equation (1) can also be used to separate different effects if the difference between the A1b and fixed-halogen simulation is used for ΔX . This is opposed to using the temporal change in a single simulation (ΔT is the difference in T due to changes in EESC, so that $m_T \Delta T$ reflects the change in O_3 caused by the T feedback). Figure 8b compares the difference in O_3 at 2.9 hPa between the A1b and fixed-halogen simulation with the contributions due to differences in EESC, T , NO_y , and HO_x , as well the sum of these contributions. There is, again, good agreement

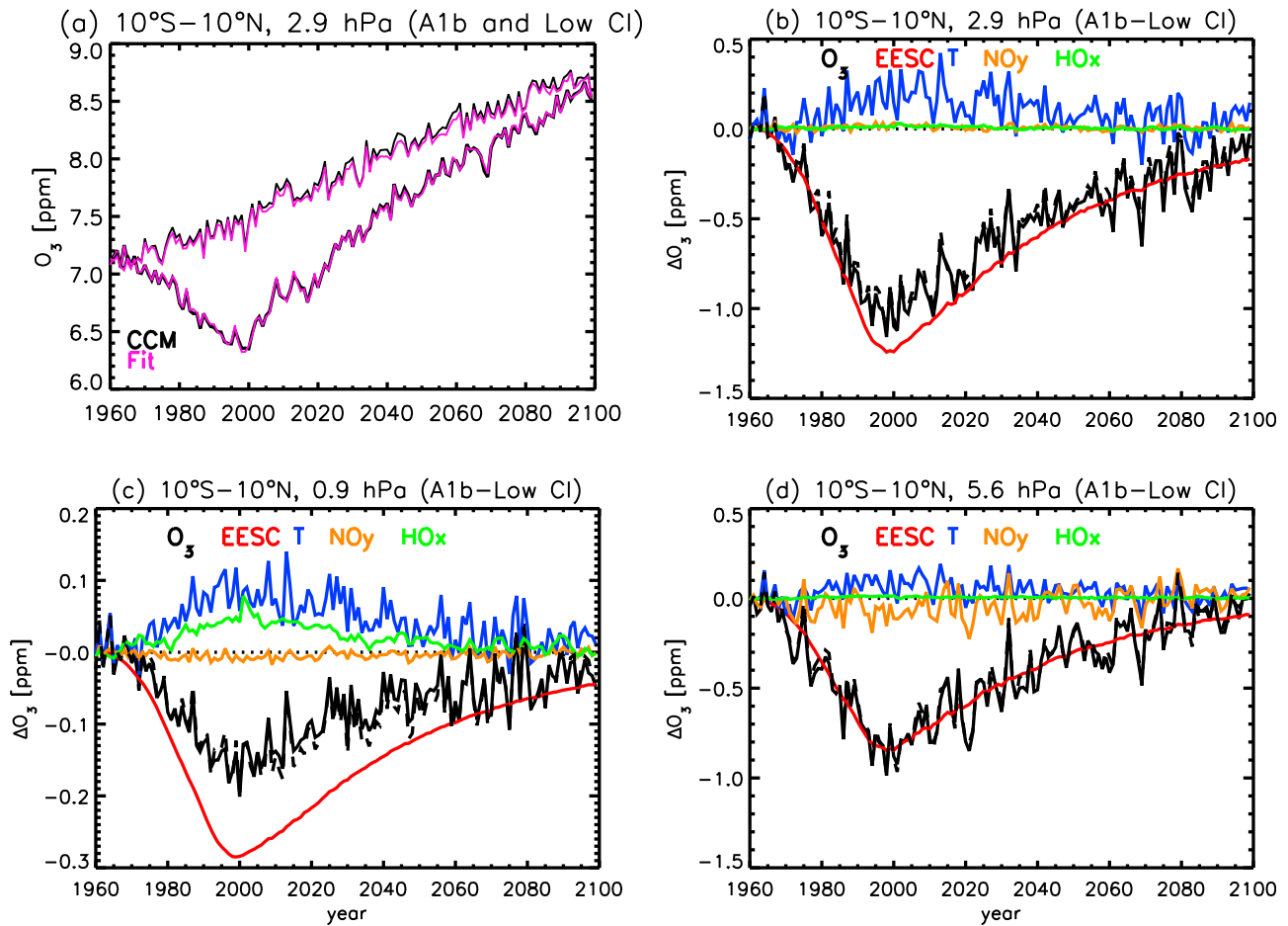
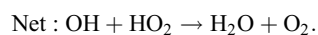
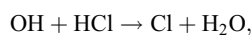
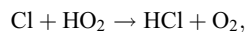


Figure 8. Evolution of ozone and from MLR for (a) 2.9 hPa, 10°S – 10°N for A1b simulation and for a fixed-halogen (Low Cl) simulation (upper curve, with the fit from A1b MLR sensitivities). (b) The difference in ozone between the A1b and fixed-halogen simulation (solid black curve) and contributions attributable to EESC (red curve), T (blue curve), NO_y (orange curve), and HO_x (green curve), as well as the sum of these contributions (dashed black curve) for 2.9 hPa, 10°S – 10°N , are shown. Also shown are the individual contributions at (c) 0.9 hPa (note the different scale) and (d) 5.6 hPa.

between the actual and reconstructed O_3 (Figure 8b, solid and dashed black curves nearly overlain). The direct impact of EESC changes (Figure 8b, red curve) dominates the change in O_3 . The blue curve (Figure 8b) represents the negative feedback due to temperature change from the direct O_3 loss caused by EESC, and it is significant. For example, in 2000 there is a total O_3 loss of ~ 1.0 ppm, which is a balance between a 1.2 ppm loss due to EESC chemical loss and a 0.2 ppm increase due to the cooling associated with this O_3 loss.

[36] At 0.9 hPa, there is not only a negative feedback from cooler temperatures, but also a negative feedback from HO_x (Figure 8c). This occurs as Cl and HCl destroy HO_x to form H_2O and O_2 [Brasseur *et al.*, 1999].



As a result of the temperature and HO_x feedback, the net ozone loss at 0.9 hPa is $\sim 50\%$ less than that expected from destruction due to EESC. Much smaller feedback is calculated at 5.6 hPa, and the direct loss due to EESC is very close to the modeled ozone loss (Figure 8d).

[37] As an additional test of the robustness of the above MLR results, we compare the coefficients m_x obtained from the MLR analysis with the sensitivities obtained from chemical box model calculations [Kawa *et al.*, 1997, 2002]. In the upper stratosphere, ozone is close to photochemical steady state, and chemical box model calculations can be used to estimate the sensitivity of ozone to the changes in different inputs.

[38] To estimate the ozone sensitivities, a reference box model calculation is first performed using the mixing ratios of chemical species, overhead ozone, and temperature for a particular location and time from the GEOS CCM simulation using the A1b scenario. In this case, we used an average 1960–2100 value to represent what was calculated in the MLR analysis. Then a series of perturbation calculations is performed, in which a single quantity (e.g., temperature) is

increased and decreased from its reference value. For EESC, Cl_y was perturbed ± 0.1 ppb, and Br_y was perturbed ± 1 ppt; temperature was perturbed ± 5 K; and NO_y was perturbed ± 1 ppb. Each simulation was run for 20 days, by which time the solution has closely approached steady state. The resulting change in ozone gives an estimate of the sensitivity of ozone to changes in this quantity, e.g., $\Delta O_3/\Delta X$ provides an estimate of sensitivity of ozone to changes in variable X . This sensitivity can then be directly compared with the coefficients m_X from equation (1).

[39] Figure 6a shows the variation in calculated steady state ozone to changes in T , EESC, and NO_y (colored crosses) for reference calculations based on simulated fields at several levels between 6.9 and 0.9 hPa for July at $2^\circ N$. Although we use annual average values for the MLR analysis, tests using other months in the chemical box model produced only small changes. These values are generally in very good agreement with the coefficients from the MLR analysis. Some disagreement is seen at 5.6 and 6.9 hPa with slightly higher EESC, NO_y , and T sensitivities from the chemical box. NO_y sensitivities are, in general, slightly larger in the box model than calculated in the MLR analysis. It is not clear, at this point, why there are some differences seen in the sensitivities between the MLR analysis and the box model. Even though there is some disagreement, overall the two methods show a similar picture and give us confidence in the MLR-based attribution of the relative contributions of different factors to the changes in ozone.

7. Conclusions

[40] In this study, we have quantified the contribution of different mechanisms to changes in the upper stratospheric ozone from 1960 to 2100 in GEOS CCM simulations and separated the direct and indirect impacts of EESC on ozone. Simulations using two different GHG scenarios (A1b and A2 from IPCC [2001]) were considered, and even though there are significant differences in the GHG concentrations in the latter half of the 21st century, there is a very similar increase in the upper stratospheric ozone over the 21st century. Isolation of different mechanisms using MLR shows that the similar ozone evolution is because of compensating effects of different mechanisms. In the A1b scenario, the increase in ozone is caused by decreases in halogenated ODSs and cooling, which is largely due to increased GHGs that alter the kinetics rate of ozone destruction, with the two mechanisms making roughly equal contributions to the ozone change. Changes in abundance of reactive nitrogen and hydrogen play only a minor role in long-term changes in the A1b scenario. In contrast, in the A2 simulation, there are significant increases in NO_y and HO_x that cause a long-term negative decrease in ozone. These decreases are largely offset by a larger positive contribution from cooler temperatures, and the ozone evolution in A2 ends up being very similar to that in A1b.

[41] The MLR analysis, together with a fixed-halogen simulation, was also used to separate the direct chemical impact and indirect feedback of EESC on ozone. The indirect impact and mechanisms were shown to vary with altitude. At 5.6 hPa, the indirect impacts are small but make significant contributions at 2.9 and 0.9 hPa. At 2.9 hPa, there is a negative feedback due to temperature increases

from the direct O_3 loss caused by EESC chemistry. This feedback is around 15% the direct EESC impact. At 0.9 hPa, there is negative feedback from temperature and from changes in HO_x due to changes in EESC, and the sum of these is around 50% of the direct EESC impact.

[42] The results presented above are based on simulations from a single model, and it will be important to consider simulations from other models. Preliminary application of the MLR method to A1b simulations from several of the CCMs examined by Eyring *et al.* [2007] yields very similar results to those presented here for the GEOS CCM (data not shown). In particular, the sensitivities are very similar, and differences in ozone evolution can be related to differences in simulated EESC, T , and NO_y fields. As well as considering other models, it will be important to consider a wider range of GHG scenarios. The very similar ozone evolution for the A1B and A2 GHG scenarios considered here might lead one to think that the ozone evolution would be similar for all likely GHG scenarios. However, the similarity between the A1B and A2 scenarios considered here occurs by the chance cancellation of differences in temperature and nitrogen and hydrogen loss cycles, and this is unlikely to be the case for all possible scenarios (e.g., for the A1F1 and B1 scenarios). It will therefore be important to perform simulations with a wider range of GHG scenarios when making projections of stratospheric ozone.

[43] This analysis of models using MLR raises the possibility of using MLR analysis to separate the contributions of changes in EESC and T to observed ozone changes. One difficulty with applying this method to data is the availability of simultaneous time series of observed ozone, EESC, T , and other quantities used in the MLR analysis. Another issue is the need to consider time periods over which the different quantities have sufficiently different temporal variations to be isolated in the MLR analysis. For the 140 years of simulation considered here, this is possible for EESC and T , but this may not be the case for shorter periods, and more analyses are needed to determine over which period data will be required to perform these analyses.

[44] **Acknowledgments.** This research was supported by the NASA MAP and NSF Large-scale Climate Dynamics programs. We thank J. Eric Nielsen for running the model simulations; Stacey Frith for helping with the model output processing; and Chang Lang, Qing Liang, and Tak Igusa for helpful comments. We also thank two anonymous reviewers for helpful comments and additions. We also thank those involved in model development at GSFC and high-performance computing resources on NASA's "Project Columbia."

References

- Austin, J., and R. J. Wilson (2006), Ensemble simulations of the decline and recovery of stratospheric ozone, *J. Geophys. Res.*, *111*, D16314, doi:10.1029/2005JD006907.
- Brasseur, G., and M. H. Hitchman (1988), Stratospheric response to trace gas perturbations: Changes in ozone and temperature distributions, *Science*, *240*, 634–637, doi:10.1126/science.240.4852.634.
- Brasseur, G. P., J. J. Orlando, and G. S. Tyndall (1999), *Atmospheric Chemistry and Global Change*, Oxford Univ. Press, Oxford, U. K.
- Chipperfield, M. P., and W. Feng (2003), Comment on "Stratospheric ozone depletion at northern mid-latitudes in the 21st century: The importance of future concentrations of greenhouse gases nitrous oxide and methane," *Geophys. Res. Lett.*, *30*(7), 1389, doi:10.1029/2002GL016353.
- Daniel, J. S., S. Solomon, R. W. Portmann, and R. R. Garcia (1999), Stratospheric ozone destruction: The importance of bromine relative to chlorine, *J. Geophys. Res.*, *104*, 23,871–23,880, doi:10.1029/1999JD00381.

- Eyring, V., et al. (2006), Assessment of temperature, trace species, and ozone in chemistry-climate model simulations of the recent past, *J. Geophys. Res.*, *111*, D22308, doi:10.1029/2006JD007327.
- Eyring, V., et al. (2007), Multimodel projections of stratospheric ozone in the 21st century, *J. Geophys. Res.*, *112*, D16303, doi:10.1029/2006JD008332.
- Haigh, J. D., and J. A. Pyle (1979), A two-dimensional calculation including atmospheric carbon dioxide and stratospheric ozone, *Nature*, *279*, 222–224, doi:10.1038/279222a0.
- Intergovernmental Panel on Climate Change (IPCC) (2001), *Contribution of Working Group I to the Third Assessment Report of the Intergovernmental Panel on Climate Change (IPCC)*, 944 pp., Cambridge Univ. Press, Cambridge, U. K.
- Jonsson, A. I., et al. (2004), Doubled CO₂-induced cooling in the middle atmosphere: Photochemical analysis of the ozone radiative feedback, *J. Geophys. Res.*, *109*, D24103, doi:10.1029/2004JD005093.
- Kawa, S. R., et al. (1997), Activation of chlorine in sulfate as inferred from aircraft observations, *J. Geophys. Res.*, *102*, 3921–3933, doi:10.1029/96JD01992.
- Kawa, S. R., R. Bevilacqua, J. J. Margitan, A. R. Douglass, M. R. Schoeberl, K. Hoppel, and B. Sen (2002), The interaction between dynamics and chemistry of ozone in the set-up phase of the Northern Hemisphere polar vortex, *J. Geophys. Res.*, *107*(D5), 8310, doi:10.1029/2001JD001527. [Printed 108(D5), 2003.]
- Li, F., R. S. Stolarski, and P. A. Newman (2009), Stratospheric ozone in the post-CFC era, *Atmos. Chem. Phys.*, *9*, 2207–2213.
- Newchurch, M. J., E.-S. Yang, D. M. Cunnold, G. C. Reinsel, J. M. Zawodny, and J. M. Russell III (2003), Evidence for slowdown in stratospheric ozone loss: First stage of ozone recovery, *J. Geophys. Res.*, *108*(D16), 4507, doi:10.1029/2003JD003471.
- Oman, L., D. W. Waugh, S. Pawson, R. S. Stolarski, and J. E. Nielsen (2008), Understanding the changes of stratospheric water vapor in coupled chemistry-climate model simulations, *J. Atmos. Sci.*, *65*, 3278–3291, doi:10.1175/2008JAS2696.1.
- Oman, L., D. W. Waugh, S. Pawson, R. S. Stolarski, and P. A. Newman (2009), On the influence of anthropogenic forcings on changes in the stratospheric mean age, *J. Geophys. Res.*, *114*, D03105, doi:10.1029/2008JD010378.
- Pawson, S., R. S. Stolarski, A. R. Douglass, P. A. Newman, J. E. Nielsen, S. M. Frith, and M. L. Gupta (2008), Goddard Earth Observing System chemistry-climate model simulations of stratospheric ozone-temperature coupling between 1950 and 2005, *J. Geophys. Res.*, *113*, D12103, doi:10.1029/2007JD009511.
- Portmann, R. W., and S. Solomon (2007), Indirect radiative forcing of the ozone layer during the 21st century, *Geophys. Res. Lett.*, *34*, L02813, doi:10.1029/2006GL028252.
- Randeniya, L. K., P. F. Vohralik, and I. C. Plumb (2002), Stratospheric ozone depletion at northern mid latitudes in the 21st century: The importance of future concentrations of greenhouse gases nitrous oxide and methane, *Geophys. Res. Lett.*, *29*(4), 1051, doi:10.1029/2001GL014295.
- Rayner, N. A., D. E. Parker, E. B. Horton, C. K. Folland, L. V. Alexander, D. P. Rowell, E. C. Kent, and A. Kaplan (2003), Global analyses of sea surface temperature, sea ice, and night marine air temperature since the late nineteenth century, *J. Geophys. Res.*, *108*(D14), 4407, doi:10.1029/2002JD002670.
- Rosenfield, J. E., and A. R. Douglass (1998), Doubled CO₂ effects on NO_y in a coupled 2-D model, *Geophys. Res. Lett.*, *25*, 4381–4384, doi:10.1029/1998GL900147.
- Rosenfield, J. E., A. R. Douglass, and D. B. Considine (2002), The impact of increasing carbon dioxide on ozone recovery, *J. Geophys. Res.*, *107*(D6), 4049, doi:10.1029/2001JD000824.
- Shepherd, T. G. (2008), Dynamics, stratospheric ozone, and climate change, *Atmos. Ocean*, *46*, 117–138, doi:10.3137/ao.460106.
- Shepherd, T. G., and A. I. Jonsson (2008), On the attribution of stratospheric ozone and temperature changes to changes in ozone-depleting substances and well-mixed greenhouse gases, *Atmos. Chem. Phys.*, *8*, 1435–1444.
- Shindell, D. T., D. Rind, and P. Lonergan (1998), Climate change and the middle atmosphere. Part IV: Ozone response to doubled CO₂, *J. Clim.*, *11*, 895–918, doi:10.1175/1520-0442(1998)011<0895:CCATMA>2.0.CO;2.
- Stolarski, R. S., A. R. Douglass, P. A. Newman, S. Pawson, and M. R. Schoeberl (2010), Relative contribution of greenhouse gases and ozone-depleting substances to temperature trends in the stratosphere: A chemistry/climate model study, *J. Clim.*, *23*, 28–42, doi:10.1175/2009JCLI2955.1.
- Waugh, D. W., L. Oman, S. R. Kawa, R. S. Stolarski, S. Pawson, A. R. Douglass, P. A. Newman, and J. E. Nielsen (2009), Impacts of climate change on stratospheric ozone recovery, *Geophys. Res. Lett.*, *36*, L03805, doi:10.1029/2008GL036223.
- World Meteorological Organization (WMO) (2003), Scientific assessment of ozone depletion: 2002, *Global Ozone Res. Monit. Proj. Rep.* 47, Geneva, Switzerland.
- World Meteorological Organization (WMO) (2007), Scientific assessment of ozone depletion: 2006, *Global Ozone Res. Monit. Proj. Rep.* 50, Geneva, Switzerland.

A. R. Douglass, S. R. Kawa, P. A. Newman, L. D. Oman, and R. S. Stolarski, Atmospheric Chemistry and Dynamics Branch, NASA Goddard Space Flight Center, Code 613.3, Greenbelt, MD 20771, USA. (luke.d.oman@nasa.gov)
 D. W. Waugh, Department of Earth and Planetary Sciences, Johns Hopkins University, Baltimore, MD 21218, USA.